Determination of the Relative Permittivity and Density within the Gas Phase and Liquid Volume Fraction Formed within the Two-Phase Region for (0.4026 CH_4 + 0.5974 C_3H_8) with a Radio Frequency Re-entrant Cavity

Mohamed E. Kandil and Kenneth N. Marsh

Department of Chemical and Process Engineering, University of Canterbury, Christchurch, New Zealand

Anthony R. H. Goodwin*

Schlumberger Technology Corporation, 125 Industrial Boulevard, Sugar Land, Texas 77478

The gas-phase relative electric permittivities, densities, and liquid drop out volumes within the two-phase envelope have been determined from measurements of the resonance frequency of the lowest order inductive−capacitance mode of a re-entrant cavity for (0.4026 CH_4 + 0.5974 C_3H_8); the dew temperatures between (315.5 and 340.4) K that correspond to dew pressures of (2.87 to 6.83) MPa for this mixture along with a description of the apparatus were reported by Kandil et al. (*J. Chem. Thermodyn.* **2005**, *37*, 684−691). The relative permittivity of the gas was determined with an uncertainty of 0.01 %. These results differed by between −(0.02 and 0.4) % from estimates obtained from the correlation reported by Harvey and Lemmon (*Int. J. Thermophys.* **2005**, *26*, 31−46) and the precise measurements of Schmidt and Moldover (*Int. J. Thermophys.* **2003**, *24,* 375− 403) for the pure components when the Oster (*J. Am. Chem. Soc.* **1946**, *68*, 2036−2041) mixing rule for total molar polarizabilities was applied. Gas densities were obtained from the relative electric permittivity with an estimated uncertainty of ±0.8 %, and the results lie within ±1.5 % of the density estimated from a cubic equation of state including crossover. The relationship between the volume of liquid in the cavity and the measured resonance frequency was established by calibration with octane. This calibration was then used to determine the liquid volume fractions, in the two-phase region, from the resonance frequency, over the range of (0.5 to 7) cm^3 in a total system volume of about 54 cm^3. The liquid volume fractions have an estimated expanded uncertainty of ±0.01. The measured liquid volume fractions agree within the expanded uncertainty with estimates obtained from the Peng−Robinson cubic equation of state with volume translation.

Introduction

The optimal recovery of naturally occurring hydrocarbon mixtures depends on knowledge of the physical properties of the porous media and the fluid contained within, including its phase boundaries, density, and viscosity. Experimental techniques are required to obtain these and other physicochemical properties that are mechanically robust and automatable and have working equations derived from physics. Recent work has demonstrated measurements of viscosity, with a vibrating wire,[1] and the detection of dew temperatures with a radio frequency re-entrant cavity;[2] both of these methods are robust and have physically based working equations.

Dew and bubble temperatures can be either determined experimentally or estimated with an equation of state; the latter typically requires as input temperature, pressure, and chemical composition, which may be obtained from, for example, gas chromatography coupled to a mass spectrometer. For retrograde condensates the dew temperatures and pressures as well as the ratio of liquid-to-gas volumes within the (liquid and gas) region, often referred to as the quality line, are arguably the most significant thermodynamic properties for the exploitation of these particular naturally occurring hydrocarbons. For these as well as other near-critical multicomponent mixtures, the dew pressures predicted, especially in the retrograde region, are often considered to be unreliable and must be measured.

* Corresponding author. E-mail: AGoodwin@slb.com. Fax: (281) 285-8071.

Experimentally, dew curves are often determined by visual observation of the first onset of liquid. Usually, but by no means always, this technique is used by industry to determine dew points. The internal dimensions of the vessels that contain the fluid are on the order of 0.1 m and, therefore, require gas sample volumes of about 1 dm^3 at the highest temperature and pressure to be studied. Phase borders obtained from visual methods often suffer systematic errors that arise from blind regions and dead volumes that, in some cases, have been reduced by refinements to the method. Nonvisual methods, which require small (on the order of 10 cm^3) samples and are also suited to automation, have been developed to determine phase borders. These include measurements of refractive index with fiber optic cables,[3] evanescent waves at gigahertz frequencies,[4] and relative permittivity.[5−9] In ref 2, dew points were determined for (0.4026 CH_4 + 0.5974 C_3H_8) from variations in resonance frequency of the *LC* mode of the re-entrant cavity with respect to temperature decrements along pseudo isochors, *L* being the inductance and *C* the capacitance.

Rigorous models for the re-entrant cavity have been reported[8] that relate the resonance frequency to the cavity dimensions, geometry, and complex electric permittivity of electrically insulating substances within the resonator. These models have been extended to electrically conducting liquids, such as water, as well as to include two *LC* lobes[10,11] and also three *LC* modes.[12] The multilobe design was primarily intended to provide the opportunity to determine, albeit over a limited

10.1021/je700053u CCC: $37.00
Published on Web 08/09/2007

range, the frequency dependence of the complex relative permittivity.

The single-lobe re-entrant cavity has also been used to measure phase boundaries,[2,8,9] to determine dipole moments[13] and density[9] in the single-phase region. The two-lobe cavity, a modified version of that reported in ref 12, has been used to determine the relative permittivity of (methane + propane) and two (methane + propane + hexane) mixtures, and the density for each was estimated by May et al.[14] May et al.[15] also reported a version of the resonator that includes a variable volume and was capable of operating isothermally, or isobarically or isochorically. The apparatus geometry was optimized to measure small liquid volume fractions in the coexisting (gas and liquid) two-phase region by the addition of a 2 mm diameter post attached to the lower surface of the bulbous portion of the lid. This post protruded into a well centered on the bottom of the outer cylinder to form a parallel plate capacitor at the bottom of the hole with a plate separation of about 0.2 mm. This additional chamber and post combination also acted as a cylindrical capacitor and, because of its location, was sensitive to liquid that either forms in or moves to the well. The apparatus was operated isothermally and used to detect phase borders and liquid volume fractions formed within the (g + l) region. Unfortunately, the apparatus suffered from a large total sample volume ≈200 cm^3 (the re-entrant cavity and chamber containing the post had a volume of about 21 cm^3),[15] and problems with fluid mixing. For (0.75 CH_4 + 0.25 C_3H_8) May et al.[15] reported densities, with an uncertainty of 0.1 %, and liquid volume fractions, with an uncertainty of 0.01 %, determined from the re-entrant cavity *LC* resonance frequency.

The operation of a cavity resonator and the determination of the (*p*, *T*) phase border from the resonance frequency of the *LC* mode was described in refs 2, 8, and 9. In ref 2, the performance of the instrument was demonstrated with measurements of the (g + l) phase border for (0.4026 CH_4 + 0.5974 C_3H_8) at temperatures between (315 and 340) K. The results compared favorably with the reported phase behavior of {(1 − *x*)CH_4 + *x*C_3H_8}. Reference 2 alluded to analyses of the resonance frequencies of the *LC* mode of the re-entrant cavity to provide the relative electric permittivity of the gas and, consequently, the density of the gas phase and phase border as well as the liquid volume fractions within the (g + l) envelope.

In a re-entrant cavity a capacitor is also formed from the separation between the bottom surface of the bulbous portion and the outer cylinder. In the resonator reported in ref 2 this separation was 5 mm and the resulting capacitance found, as will be demonstrated in this paper, to provide values of the liquid volume fractions accumulated within the bottom of the cavity; in the cavity reported by May et al.[15] this separation was about 0.5 mm.

The measured relative permittivities have been compared with estimates obtained from correlations of the relative permittivity of pure gases reported by Harvey and Lemmon[16] and Schmidt and Moldover,[17] combined with mixing rules for the total molar polarizability reported by Harvey and Prausnitz[18] and Oster,[19] respectively. The densities are compared with estimates obtained from five equations of state, and the liquid volume fractions, within the two-phase region, are compared with values obtained from three equations of state.

Working Equations

When both the capacitor and the inductor of the re-entrant cavity are immersed in fluid, to first order, the resonance frequency is given by

$$f \approx \{4\pi^2 \mu_r L(p=0)\epsilon' C(p=0)\}^{-1/2} \quad (1)$$

where μ_r is the relative magnetic permeability, $\mathscr{R}(\epsilon_r) \equiv \epsilon'$ is the relative electric permittivity of the fluid, and $L(p = 0)$ and $C(p = 0)$ are the inductance and capacitance at $p = 0$, respectively. Most dielectric fluids are diamagnetic, and the product $\mu_r\epsilon'$ is well approximated by ϵ'. If this approximation was used to determine the polarizability of liquid CO_2 at $T =$ 293.15 K, the relative error in ϵ_r would be $\approx \pm 10^{-5}$. For the gases studied in the work this assumption results in a negligible additional uncertainty.[20] The simple model of eq 1 suffices for the purpose of determining phase boundaries from measurements of the resonance frequency along an isochore.[2,8,9] However, this approach provides an inadequate representation of the system when the measured resonance frequency is to be interpreted to provide the relative electric permittivity ϵ_r and from that the amount-of-substance density ρ_n. To obtain ϵ_r and then ρ_n requires all products L_iC_i of the cavity be accounted for including those arising from fringing fields, induction effects for the capacitors, and capacitive effects for the inductors, and contribution from the 5 mm gap at the bottom of the cavity. A waveguide model has been reported to accommodate all of these effects[8] and used to determine relative electric permittivities and dipole moments.[8,13] In refs 8 and 13 the capacitance associated with fringing fields at the upper ends of the capacitive section C' were estimated with the methods described by Marcuwitz.[21]

Determination of Relative Electric Permittivity. An alternative to the waveguide model reported in ref 8 is a lumped-parameter (equivalent circuit) model reported by Hamelin et al.[10,11] that relates the complex electric permittivity ϵ_r to the measured resonant frequency f_r through

$$\epsilon_r = \left(\frac{f_0 + ig_0}{f_r + ig}\right)^2 \left(\frac{1 + (-1 + i)Q^{-1}}{1 + (-1 + i){Q_0}^{-1}}\right) \quad (2)$$

where the resonance quality factor $Q = f_r/(2g)$ and the subscript 0 denotes values obtained when the resonator is evacuated. Equation 2 has been used to determine the complex relative permittivity ϵ_r when f_r, g, f_0, and g_0 have been measured with a weakly coupled resonator filled with fluid for which the electrical conductivity is small and Q is sufficiently large so terms in Q^{-2} are rendered negligible.[11,20] The real part of the complex quantity ϵ_r ($\equiv \epsilon' - i\epsilon''$), which can depend on frequency, is the dielectric constant ϵ', whereas the imaginary part, $\epsilon'' = \sigma/(\omega\epsilon_0)$ accounts for electrical dissipation within the dielectric fluid of electrical conductivity σ. Equation 2 was derived by assuming both σ and ϵ_r are independent of frequency. When $\sigma \ll 1$, then $\epsilon'/\epsilon'' \gg 1$ and simple measurements of frequency suffice because $\mathscr{R}(\epsilon_r) \equiv \epsilon'$; eq 2 of ref 15 gives the low-loss approximation to eq 2.

The parameters f_0 and g_0 of eq 2 account for dilation of the dimensions of the cavity resulting from variations in temperature and pressure; when the electromagnetic cavity that forms the resonator also acts as the pressure vessel, as it does in our apparatus, the compressibility of the wall material is significant. The parameters also account for the variations in spatial distribution of the electromagnetic field within the cavity that occurs between the evacuated and fluid-filled resonator. The corrections can be determined from measurements of the complex resonant frequency of the cavity when evacuated and filled with a fluid for which the thermophysical properties are known over a range of temperatures and pressures. The values of f_r and g obtained when the cavity is filled with fluid can be substituted in eq 2 to obtain the relative permittivity ϵ_r.

The parameters f_0 and g_0 of eq 2 may be represented by[12]

$$f_0 = f_{00}\{1 - \alpha(T - T_{ref})\}(1 + \gamma p) \quad (3)$$

and

$$g_0 = g_{00} \quad (4)$$

where the terms $\{1 - \alpha(T - T_{ref})\}$ and $(1 + \gamma p)$ in eq 3 are factors that account for thermal expansion and dilation, respectively, and include the linear thermal expansion coefficient α and a parameter, γ, related to the elastic properties of the resonator. In eq 3 T_{ref} is the temperature at which the parameters were determined, p the pressure, and f_{00} the resonance frequency when the cavity was evacuated, whereas in eq 4 g_{00} is the resonance line width in vacuum. Measurements of the resonance frequency when the cavity is filled with a substance for which ϵ_r is known are used to determine γ by minimizing the difference between ϵ_r, obtained from eqs 2, 3, and 4, and the accepted literature value. This procedure is adopted because the elastic properties are required for a resonator formed from two parts that are bolted together.

Determination of Amount-of-Substance Density from Relative Electric Permittivity. Determination of the amount of substance density ρ_n from measurements of the relative electric permittivity requires a relationship between these properties. Unfortunately, there is no universally obeyed relationship between the relative electric permittivity ϵ_r $[=\mathscr{R}(\epsilon_r)=\epsilon']$ and ρ_n. At moderate densities (<0.01 mol·cm^{-3}) the total molar electric polarizability $\mathscr{P}(\rho, T)$ can be given by

$$\mathscr{P}(\rho_n, T) = \frac{\epsilon_r - 1}{\epsilon_r + 2}\frac{1}{\rho_n} = A_\epsilon(1 + b\rho_n + c{\rho_n}^2 + ...) \quad (5)$$

where A_ϵ, b, c, ..., are the first, second, third, ..., permittivity (dielectric) virial coefficients. In eq 5 A_ϵ is the molar polarizability that arises from individual molecules in the absence of intermolecular interactions and is given by the Debye expression.

$$A_\epsilon = A_\epsilon(\text{elec}) + A_\epsilon(\text{atom}) + \frac{N_A}{9\epsilon_0 k}\frac{{\mu_D}^2}{T} \quad (6)$$

In eq 6 A_ϵ(elec) is the electronic contribution (which can be determined from measurements of refractive index), A_ϵ(atom) the atomic contribution, N_A Avogadro's constant, ϵ_0 the electric constant (permittivity of free space), k Boltzmann's constant, and μ_D the permanent dipole moment, which is also a function of temperature.

For nonpolar molecules ($\mu_D = 0$) eqs 5 and 6 can be approximated by the Clausius−Mossotti equation

$$\frac{\epsilon_r - 1}{\epsilon_r + 2}\frac{1}{\rho_n} \approx \mathscr{P}_{CM} \quad (7)$$

where $\mathscr{P}_{CM}$ is a constant. Equation 7 can be applied to nonpolar fluids, such as methane, for which $\mathscr{P}_{CM}$ changes by about 0.7% when the amount-of-substance density varies from (0.002 to 0.03) mol·cm^{-3} at temperatures between (100 and 300) K and pressures in the range of (2 to 35) MPa.[22] For the molecules and temperatures of interest here, rotational effects provide a linear increase of A_ϵ (and $\mathscr{P}_{CM}$) with increasing temperature.[23] For nonpolar molecules, such as butane, $\mathscr{P}_{CM}$ decreases with increasing density (and decreasing temperature) for liquid densities that range from critical to the triple point.[24] However, for the weakly polar compounds such as propane[24,25] and 2-methylpropane,[26] the $\mathscr{P}_{CM}$ increases rapidly, proportional to ${\mu_D}^2/T$, at low temperatures (or high densities) for the liquid along the saturation curve. Measurements of both density, obtained with a magnetic suspension densimeter, and relative electric permittivity, determined with an audio frequency concentric cylinder capacitor, have confirmed the utility and bounds of eq 7.[24,26]

For polar fluids more complex expressions for the total molar polarizability have been proposed, and these are discussed by Böttcher.[27] One of these expressions is the equation of Kirkwood and Onsager:[28]

$$\frac{(\epsilon_r - 1)(2\epsilon_r + 1)}{9\epsilon_r}\frac{1}{\rho_n} \approx \mathscr{P}_{KW} \quad (8)$$

The factors $\mathscr{P}_{CM}$ and $\mathscr{P}_{KW}$ are in close agreement when, as is the case in this work, $\epsilon_r < 2$; for $\epsilon_r = 1.5$, $\mathscr{P}_{CM}$ and $\mathscr{P}_{KW}$ differ relatively by about $5\cdot10^{-3}$. Significant differences between the factors $\mathscr{P}_{CM}$ and $\mathscr{P}_{KW}$ are found for fluids containing components with very high relative permittivity and correspondingly large dipole moments, such as water.[18,19]

The molar polarizability of liquid mixtures can be estimated from Oster's rule,[19] which for a binary mixture

$$(1 - x)\text{A} + x\text{B} \quad (9)$$

is

$$\frac{\mathscr{P}(x, T, p)}{\rho_n(x, T, p)} = (1 - x)\frac{\mathscr{P}(\text{A}, T, p)}{\rho_n(\text{A}, T, p)} + x\frac{\mathscr{P}(\text{B}, T, p)}{\rho_n(\text{B}, T, p)} \quad (10)$$

Equation 10 becomes a linear mixing rule when the excess volume of mixing at T and p is zero:[29]

$$\mathscr{P}(x, p, T) = (1 - x)\mathscr{P}(\text{A}, p, T) + x\mathscr{P}(\text{B}, p, T) \quad (11)$$

Oster's rule is effectively a mixing of pure-component total polarizations at constant temperature and pressure. For liquid mixtures eq 11 provides values of $\mathscr{P}(x, p, T)$ within ±0.2 % of the measured values for liquid mixtures except those containing polar compounds.[14,30] Nevertheless, other workers[31] have combined eqs 7 and 11 to obtain liquid densities with claimed uncertainties of 0.1 % even for mixtures including polar components, admittedly after more carefully accounting for the density and composition dependencies of $\mathscr{P}(x, p, T)$ and $\mathscr{P}_{CM}$.

May et al.[14] measured ϵ_r, with a re-entrant cavity,[14] and simultaneously ρ_n, with a dual sinker densimeter,[32] for one binary mixture of methane, propane, and hexane and determined $\mathscr{P}(x, p, T)$ from eq 7. In ref 14 the measured $\mathscr{P}(x, p, T)$ were compared with values estimated from eq 11 based on the known $\mathscr{P}$ for the pure components[33,34] obtained from eq 5, and differences of between (0.1 and 0.6) % in $\mathscr{P}(x, p, T)$ were observed, which had an uncertainty of ±0.2 %.

In general, use of eq 10 (or eq 11) to determine $\mathscr{P}(x, p, T)$ could result in a systematic error in the density because the critical conditions of the components may differ significantly, and at the temperature and pressure of interest one of the components could be normally a liquid as a pure substance.[18] To overcome the limitations of Oster's rule[19] (eq 11) Harvey and Prausnitz[18] proposed the total molar polarization be obtained by mixing the pure component $\mathscr{P}$ at constant temperature and reduced density according to

$$\mathscr{P}(x, T, p) = \frac{(1-x)V_m^c(A)}{\{(1-x)V_m^c(A) + xV_m^c(B)\}} \mathscr{P}[A, \rho_r(x)/V_m^c(A)] + \frac{xV_m^c(B)}{\{(1-x)V_m^c(A) + xV_m^c(B)\}} \mathscr{P}[B, \rho_r(x)/V_m^c(B)] \quad (12)$$

In eq 12 V_m^c is the critical molar volume and the reduced density $\rho_r(x)$ is given by

$$\rho_r(x) = \rho(x)\left\{\frac{(1-x)}{\rho^c(A)} + \frac{x}{\rho^c(B)}\right\} \quad (13)$$

where $\rho(x)$ is the molar density of the mixture and ρ^c the critical density for each component. Equations 12 and 13 were used by Harvey and Lemmon[16] for natural gas mixtures.

For polar fluids the $\rho_n(x, T, p)$ for a binary mixture (eq 9) can be obtained from

$$\rho_n(x, T, p) = \frac{[\epsilon_r(x, T, p) - 1][2\epsilon_r(x, T, p) + 1]}{9\epsilon_r(x, T, p)} \frac{1}{\mathscr{P}(x, T, p)} \quad (14)$$

with measurements of the relative permittivity $\epsilon_r(x, T, p)$ and an estimate of the total molar polarizability $\mathscr{P}(x, T, p)$ of the mixture that is determined from values of $\mathscr{P}(A, p, T)$ and $\mathscr{P}(B, p, T)$. The $\mathscr{P}(x, T, p)$ can be estimated with Oster's rule,[19] eq 10, assuming it applies to gases or eq 11 when it is also assumed there is zero volume change upon mixing or eqs 12 and 14 when both the critical density and volume of the pure components are known. For nonpolar fluids eq 7 with eq 11 has been adopted to determine density in refs 8, 9, and 15. Values of $\mathscr{P}(A, p, T)$ and $\mathscr{P}(B, p, T)$ can be obtained from measurements or independent sources including correlations of ϵ_r.

Correlations of ϵ_r(g) for Pure Components. Schmidt and Moldover[17] measured the relative permittivity of eight gases, including methane and propane, with a toroidal cross capacitor with $\delta\epsilon_r \approx 0.5 \cdot 10^{-6}$. For methane the measurements were at temperatures of (273.17 and 302.45) K at pressure below 7 MPa, whereas those of propane were at temperatures of (273.17, 295.65, and 313.15) K and pressures of less than 0.8 MPa. The vapor pressure of propane limited the maximum pressure and the amount of substance densities to ≤ 0.0004 mol·cm^{-3}. The measured $\epsilon_r(p, T)$ values were converted to $\epsilon_r(\rho_n, T)$ using the Setzmann and Wagner[35] equation of state for methane, based on diverse thermodynamic measurements, and a virial equation of state, derived from precise sound speed measurements at low densities by Trusler,[36] for propane. Solely these values of $\epsilon_r(\rho_n, T)$ were fit to eq 5 truncated after $c\rho_n^2$ for methane and after $b\rho_n$, combined with eq 6, for propane; our analysis shows eq 10 of ref 17 is incorrect. The fractional standard deviations of the fits were about 10^{-6}. The contribution of the dipole moment to the total polarizability of propane was never more than 0.14 cm^3·mol^{-1} in 16.1 cm^3·mol^{-1} (about 0.9 %).

Harvey and Lemmon[16] have correlated measurements of $\epsilon_r(p, T)$, converted to $\epsilon_r(\rho_n, T)$, from the literature over a wider range of states with the total molar polarizability and a modified form of eq 5:

$$\mathscr{P}/\rho_n = A_\epsilon(T) + A_\mu/T + B_\epsilon(T)\rho_n + C(T)\rho_n^D \quad (15)$$

In ref 16 empirical functions of temperature were used to represent A_ϵ, B_ϵ, C, and $A_\mu = N_A\mu_D^2/(9\epsilon_0 k)$. The $\mathscr{P}$ was related to ϵ_r with eq 8 for propane and with eq 7 for methane, and the density of methane was obtained from ref 35, whereas that of propane was obtained from Span and Wagner.[37] To verify the operation of their correlation, Harvey and Lemmon[16] compared the predicted ϵ_r with the values reported by May et al.[14] for (methane + propane) and found $100\Delta\epsilon_r \leq 0.05$, which is about 2.5 times the expanded uncertainty of the measurements. This is a best case comparison because the density of the mixture was measured simultaneously by May et al.[32] When the estimates were obtained with Oster's rule[19] (eq 11), the deviations were systematic and at the highest density of ≈0.005 mol·cm^{-3} found to be $100\Delta\epsilon_r \approx 0.2$.[16] The correlation of Harvey and Lemmon[16] requires only the density of the mixture.

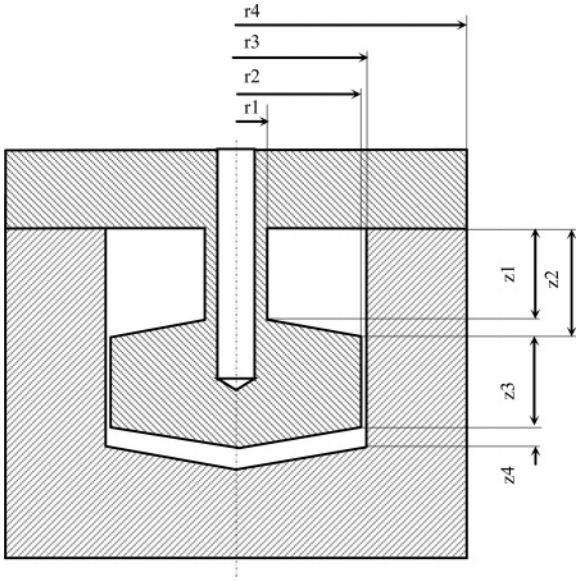

Figure 1. Schematic cross-section through the resonator with dimensions r1 = 6 mm, r2 = 24 mm, r3 = 25 mm, r4 = 45 mm, z1 = 20 mm, z2 = 23.5 mm, z3 = 20 mm, and z4 = 5 mm.[2]

Calculation of Liquid Volume Fraction. The liquid volume fraction can be calculated in the two-phase region (liquid + gas) with a normalized function

$$\Phi = \frac{[\epsilon_r(x, T, p) - \epsilon_r(g, T, p)]}{[\epsilon_r(1, T, p) - \epsilon_r(g, T, p)]} \quad (16)$$

where $\epsilon_r(x, p, T)$ is the measured relative electric permittivity for the mixture at pressure p and temperature T at which the resonance frequency had been measured within the two-phase region, $\epsilon_r(g, T, p)$ is the relative permittivity of the gas, and $\epsilon_r(1, T, p)$ is the relative permittivity of the liquid at the same p and T. Equation 16 is identical to eq 4 of ref 15.

Apparatus, Experimental Procedures, and Calibration

The apparatus has been described in detail elsewhere,[2] and only the features important to interpreting the results reported are elaborated below. The apparatus consisted of a re-entrant resonator, similar to that reported by Goodwin et al.,[8,9] a magnetically activated circulation pump, and a differential pressure gauge, all mounted within a circulated air thermostat for which the temperature was controlled to $<\pm 3$ mK. The re-entrant cavity was formed in two parts with the geometry required to both form the *LC* resonator and act as a pressure vessel capable of operating at temperatures up to 470 K and pressures below 20 MPa. When assembled, the resonator, with dimensions shown in Figure 1, has an internal volume of about 54 cm^3, and an annular gap of about 1 mm separated the bulbous extension and the inner surface of the canister. All internal surfaces exposed to fluid were machined and polished to a mirror finish so that the surface defects were <1 μm with an

average surface roughness of 0.25 μm. The lower surfaces of both the canister and bulbous portion were angled to enhance drainage when oriented in a gravitational field; it also acted as a parallel plate capacitor. Sample entered the cavity through the lid and, when the metering valve in the canister base was open, exited through the base and into the circulation pump that pushes fluid through the differential pressure gauge to the inlet within the top of the cavity. When the metering valve was closed, the valve stem was reproducibly positioned flush with the inner surface with a vernier handle. These features were designed to prevent any possibility of introducing dead volume in this section so that the ratio of the gas-to-liquid volumes within the two-phase region could be determined with this apparatus.

The procedure described in ref 2 was used to determine the complex resonant frequency $f_r + ig$, where g is the line width, with a relative standard uncertainty of $\delta f/f \approx 2 \cdot 10^{-7}$. The uncertainty in the measured dew temperature was estimated in ref 2 to be ≈0.06 K, and the corresponding uncertainty in the phase boundary pressure was assumed to contribute <0.005 MPa. The $\{(1 - x)CH_4 + xC_3H_8\}$ mixture was prepared as described in ref 2 with $x = 0.5974 \pm 0.0013$. The resolution and uncertainty with which temperature, pressure, and frequency could be measured were far less than the uncertainty in the mole fraction of the mixture, which dominates the error in the (p, ρ, T) phase border and liquid volume fractions. Octane was used to determine the resonators' internal volume. The octane, supplied by Koch-Light, was of puriss grade with a mass fraction purity of 0.99 as determined by GLC.

Calibration of the Cavity for the Determination of ϵ_r. To determine complex relative electric permittivity ϵ_r from eqs 2 and 3 requires values for the parameters α, γ, f_{00}, and g_{00} of eq 3. The re-entrant cavity was constructed from type 316 stainless steel for which $\alpha \approx 15.9 \cdot 10^{-6}$ K^{-1}.[38] The γ, f_{00}, and g_{00} values were obtained from measurements of the resonant frequencies when the cavity was evacuated and also filled with methane at six, equally spaced, pressures between (3 and 9) MPa on an isotherm at a temperature of 323.15 K. This temperature corresponded with a temperature at which Moldover and Buckley[34] had reported the relative permittivity of methane determined from capacitance measurements with a toroidal cross capacitor, a technique with systematic errors entirely different from those of a radio frequency re-entrant cavity. To estimate $\mathscr{R}(\epsilon_r)$ ($\equiv \epsilon' \equiv \epsilon_r$) from ref 34 at our experimental temperatures and pressures, the density of methane was required, and this was obtained from the correlation of Setzmann and Wagner[35] as implemented within the NIST REFPROP database.[39] The parameters of eq 3 were determined by regression to minimize the difference between the ϵ_r obtained from eqs 2 and 3, with the frequencies obtained in vacuum and methane, and the ϵ_r reported in ref 34 with the results $f_{00} = 344.553$ MHz, $\gamma = 104 \cdot 10^{-6}$ MPa^{-1}, and $g_{00} = 0.585$ MHz. On the basis of this calibration, the fractional expanded uncertainty in the relative permittivity $\delta\epsilon_r/\epsilon_r$ obtained from the measured frequency was estimated to be about 10^{-4}. Both the density and liquid volume fractions were calculated from the measured relative permittivity.

Calibration of the ϵ_r(I) Obtained from the Resonance Frequency as a Function of Liquid Volume. To obtain the liquid volume fraction within the (1 + g) region requires knowledge of the volume of each section of the cavity, the total resonator volume V, which was determined from the dimensions of the canister and bulbous portion shown in Figure 1, and the function Φ of eq 16 that relates the liquid volume within the cavity to the relative permittivity and thus the resonance frequency of the cavity. In this work, the function Φ was determined from measurements of the cavity resonance frequency, from which the effective ϵ_r was obtained, as a function of the volume of liquid octane within the cavity and assuming the electric permittivities of eq 16 were given by $\epsilon_r(C_8H_{18}, g, 293\ K, 0.1\ MPa) = 1.0008$ and $\epsilon_r(C_8H_{18}, l, 293\ K, 0.1\ MPa) = 1.9476$.[34,40−42]

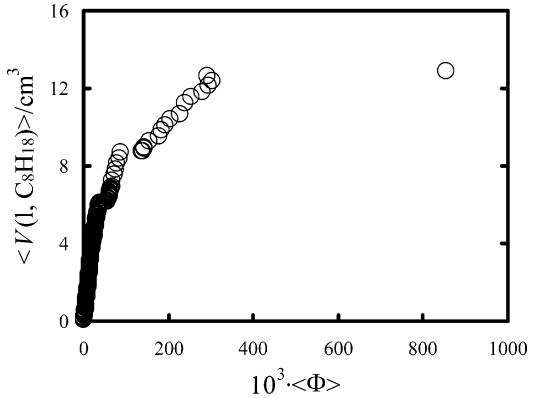

Figure 2. Mean volume of liquid displaced into the cavity $<V(l, C_8H_{18})>$ as a function of the mean $<\Phi>$ obtained from eq 16: ○, obtained with octane at a temperature of 292.4 K and a pressure of 0.1 MPa, where the gas above the liquid is a mixture of octane and air.

During the calibration, liquid octane was fed from the bottom of the cavity into the capacitor formed between the lower surface of the bulbous portion and the bottom of the pressure vessel. After each injection of ≈0.06 cm^3 multiple measurements of the resonance frequency were obtained. The mean values of the liquid volume $<V(l)>$ determined, at each condition, that include V(l) from (0.06 to 12.9) cm^3 and $10^3\Phi$ from (0.2 to 854) are shown in Figure 2 as a function of the mean $<\Phi>$. The results determine the response of the cavity to liquid of $\epsilon_r \approx 2$ residing in the lower capacitor. If a liquid of volume 12.4 cm^3 were injected into the cavity, oriented as shown in Figure 1, the liquid-to-gas interface would reside at the height z4, of Figure 1, from the base of the resonator; on the basis of the dimensions shown in Figure 1, the total internal volume of the cavity was 53.97 cm^3.

Nevertheless, it is clear from Figure 2 that discontinuities occur at $10^3\Phi \approx 37$ and also $10^3\Phi \approx 88$ that correspond with $<V(l)> \approx 6$ cm^3 and $<V(l)> \approx 8.7$ cm^3, respectively. The expectation was for the first discontinuity to arise from liquid touching the lowest protrusion of the bulbous portion and the second from liquid reaching height z4, shown in Figure 1. However, the volumes for each geometrical portion of the cavity, shown in Figure 3, are greater than the volumes assigned to each discontinuity. Interfacial tension provides one plausible explanation for the appearance of these discontinuities at the V(l): liquid enters the cavity from the bottom, and the level of the liquid in the lower capacitor increases until, when it is close to a point at the base of the central bulbous portion, interfacial tension forms a meniscus that distorts the values of Φ. Although neither measurement nor rigorous calculation were performed to verify this conjecture, additional, albeit anecdotal, support was obtained from preliminary experiments performed to determine the resonator's response as a function of V(l), where the liquid octane was admitted from the upper inlet. In this case, the liquid runs down from the top over the central bulbous portion, and interfacial tension forms a drop that protrudes from the lowest point of the bulbous portion. The level of the liquid in the lower capacitor increases until it meets the drop. In these measurements, not reported here, a discontinuity in V(l) as a

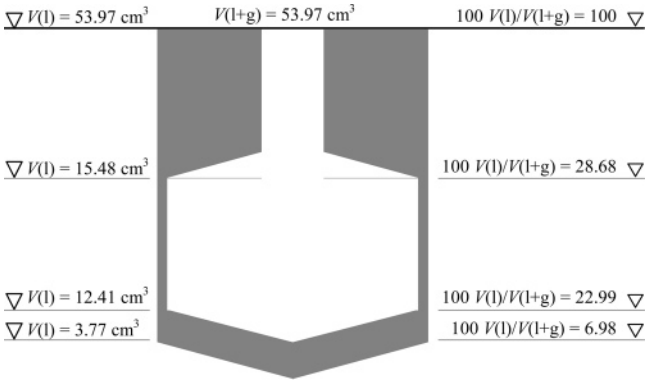

Figure 3. Liquid volumes $V(l)$ along with the ratio to total volume $V(l+g)$ at each major variation in geometry of the re-entrant cavity.

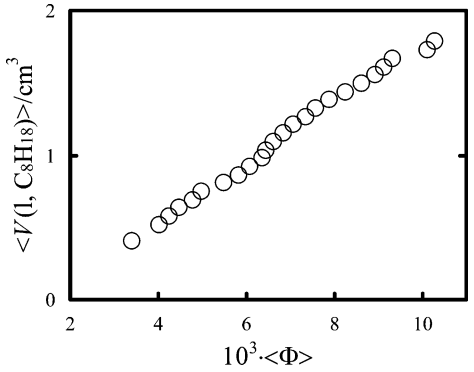

Figure 4. Mean volume of liquid displaced into the cavity $\langle V(l, C_8H_{18})\rangle$ as a function of the mean $10^3\langle\Phi\rangle$, obtained from eq 16, for $\langle V(l, C_8H_{18})\rangle = (0.4 \text{ to } 1.8)$ cm^3, which is significant to this work: ○, obtained with octane at a temperature of 292.4 K and a pressure of 0.1 MPa, where the gas above the liquid is a mixture of octane and air.

function of Φ was observed at a liquid height of about 3 mm, which is about 2 mm below the lowest point on the bulbous portion and another at a liquid level of 5 mm when the liquid level contacts with the tip of the bulb. In our preliminary experiments, when fluid flowed from the top of the cavity, in the $\langle V(l)\rangle$ range of (0.4 to 1.8) cm^3, the dependence on Φ was not a smooth linear function consistent with the effect of interfacial tension.

For ($0.4026CH_4 + 0.5974C_3H_8$) the measured volume of liquid formed within the two-phase region is <4 cm^3, and of these 38 measurements 34 have $V(l) < 2$ cm^3; this guided the range of measurements used for the calibration with octane. There are 58 measurements of $10^3\Phi$ for $\langle V(l)\rangle$ from (0.4 to 1.8) cm^3 with octane and, as shown in Figure 4, with an ordinate expanded by a factor of 8 compared with Figure 2, are a smooth linear function that may be represented by

$$V(l)/\text{cm}^3 = 214.978\Phi \qquad (17)$$

with a standard deviation of $\sigma\{V(l)\} = 0.028$ cm^3. The relative fractional deviations of the experimental values of $\langle V(l)\rangle$ from eq 17 are, as shown in Figure 5, random and typically within the estimated standard uncertainty of $100\langle V(l)\rangle/V(l) = \pm 2.7$, also illustrated in Figure 5. Had the measurements of $V(l)$ included in the regression analysis increased to 4.1 cm^3, the coefficient of eq 17, and therefore the calculated V(l), would decrease by 0.9 %, whereas the standard deviation of the fit was ≈0.04 cm^3. For $V(l) = 4$ cm^3, the worst case, this corresponds to $\delta\{V(l)/V(1+g)\} \approx 0.005$.

Uncertainty in the Liquid Volume Fraction. The minimum detectable liquid volume increment (or the liquid volume threshold) is determined by the uncertainty of the resonance frequency that is used to distinguish the onset of condensation. As liquid first forms in the lower section of the cavity, $dV(l)/df_r \approx 0.6$ cm^3·MHz^{-1} and is almost a linear function of resonance frequency over a volume increment of 0.5 cm^3. The estimated uncertainty in the resonance frequency $\delta f_r \approx 0.002$ MHz, and hence the minimum volume that can be detected, is ≈0.001 cm^3. This implies a minimum detectable liquid volume fraction $V(l)/V(l+g) \approx 4\cdot10^{-5}$, where $V(l)$ is the liquid volume in a resonator of total volume available to the gas and liquid of $V(g+l)$.

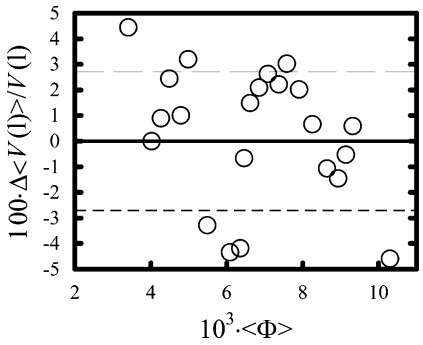

Figure 5. Relative difference $\Delta\langle V(l)\rangle/\langle V(l)\rangle = \{\langle V(l, \text{exptl})\rangle - V(l, \text{calcd})\}/V(l, \text{calcd})$ of the experimental mean liquid volume displaced into the cavity $\langle V(l, \text{exptl})\rangle$ from the volume $V(l, \text{calcd})$ estimated from eq 17 as a function of the mean $10^3\langle\Phi\rangle$ for $V(l, C_8H_{18}) = (0.4 \text{ to } 1.8)$ cm^3, which is significant to this work: ○, obtained with octane at a temperature of 292.4 K and a pressure of 0.1 MPa, where the gas above the liquid is a mixture of octane and air. The dashed lines represent $\sigma\{V(l)\}/\langle V(l)\rangle = 0.027$, where $\sigma\{V(l)\}$ is the standard deviation of the fit to obtain eq 17.

Fortunately, even at the minimum detectable liquid volume of $V(l)/V(l+g) \approx 4\cdot10^{-5}$, the depth of the liquid in the cavity was estimated to be ≈0.5 mm, which is about 500 times greater than the surface roughness of the cavity. This liquid depth effectively eliminates a systematic error arising from an uneven distribution of the liquid that would occur if the liquid level approaches the height of surface roughness. Furthermore, the open conical space at the bottom of the cavity reduces the possibility of inclusion of any gases that could be trapped within dead volumes.[15]

The major sources of error in $V(l)/V(l+g)$ arise from the calibration and the uncertainty in ϵ_r of eq 16. To determine the function Φ, a liquid volume increment of ≈0.06 cm^3 was used and, with a resonator of internal volume ≈54 cm^3, gives $\delta\{V(l)/V(l+g)\} \approx 0.001$. Equation 17 represented the results with $\sigma\{V(l)\} = 0.028$ cm^3 that contributes $\delta\{V(l)/V(l+g)\} = 0.0005$. The calculation of $V(l)/V(l+g)$ also requires values of $\epsilon_r(l+g)$ and $\epsilon_r(g)$ that are both obtained from the measurements with an estimated standard ($k = 1$) uncertainty of $\delta\epsilon_r/\epsilon_r = 0.003$ and $\epsilon_r(l)$ obtained from ref 16 with $\delta\epsilon_r/\epsilon_r = 0.002$. Combining these three sources of uncertainty in quadrature results in an expanded ($k = 2$) uncertainty $\delta\{V(l)/V(l+g)\} \approx 0.008$.

Results and Discussion

Relative Electric Permittivity. The $\epsilon_r(g)$ values for ($0.4026\ CH_4 + 0.5974\ C_3H_8$) are listed in Table 1. The estimated expanded ($k = 2$) uncertainty $\delta\epsilon_r = \pm 0.0003$; this value was obtained from the calibration measurements with methane and includes the uncertainty of the resonance frequency measurements.

Unfortunately, we are not aware of independent measurements of the relative permittivity of ($0.4026\ CH_4 + 0.5974\ C_3H_8$) with which to compare our results. Consequently, we compared our measured values of ϵ_r with those obtained from the following

Table 1. Gas-Phase Amount of Substance Density ρ_n and Relative Permittivity ϵ_r of the Gas at Pressure p and Temperature T for (0.4026 CH_4 + 0.5974 C_3H_8). The Amount of Substance Density ρ_n(SM) Obtained from the Measured ϵ_r Using Eq 7 for Mixtures with $\mathscr{P}_{CM} = \mathscr{P}(x, \rho_n, T)$ Estimated with Schmidt and Moldover[17] Values of $\mathscr{P}(\rho_n, T)$ for Pure CH_4 and C_3H_8 Calculated from Eqs 5, 6, and 7 and $\rho_n CH_4$ of Ref 35 and $\rho_n C_3H_8$ of Ref 36 Combined According to Oster's Rule.[19] The ρ_n(HL) Was Obtained from the Measured ϵ_r Using Eq 14 with $\mathscr{P}(x, \rho_n, T)$ Estimated with the Harvey and Lemmon[16] Values of $\mathscr{P}(\rho_n, T)$ for Pure CH_4 and C_3H_8 and Eqs 5, 6, and 8

T / K	p / MPa	ϵ_r	ρ_n(SM) / mol·cm^{-3}	ρ_n(g)(HL) / mol·cm^{-3}
343.48	7.0252	1.176192	0.004518	0.004439
340.07	5.7063	1.125448	0.003271	0.003226
338.64	5.3864	1.114861	0.003006	0.002967
336.73	4.9952	1.103135	0.002710	0.002678
334.27	4.6135	1.092567	0.002442	0.002415
332.18	4.3034	1.084491	0.002235	0.002213
329.11	3.9365	1.075498	0.002004	0.001986
325.96	3.6863	1.070319	0.001870	0.001854
323.90	3.3986	1.063308	0.001688	0.001675
318.40	2.9249	1.053563	0.001433	0.001424

two correlations: (1) the total molar polarizability for each pure component determined with the parameters reported by Schmidt and Moldover[17] (eqs 5, 6, and 7) with densities from refs 35 and 36 combined with Oster's mixing rule[19] (eq 11); and (2) the Harvey and Lemmon[16] correlation that includes eqs 8, 12, and 13 with the critical molar volumes of $V^c_m(CH_4) = 200$ cm^3·mol^{-1} and $V^c_m(C_3H_8) = 98.629$ cm^3·mol^{-1} from refs 35 and 37, respectively. For both methods, the density of the mixture is required to determine ϵ_r, and this was arbitrarily obtained from the following two sources: the Soave−Redlich−Kwong[43] cubic equation of state with binary interaction parameters $k_{ij} = 0.012$ as implemented in HYSYS[44] and the cubic crossover equation of state by Kiselev;[45,46] these two equations of state, and the values of density obtained from them, will be discussed in the following section. Over the temperature and pressure ranges listed in Table 1 the difference between the densities predicted by these two methods increased with increasing temperature from (1 and 3.4) %.

If the density of the mixture had been estimated with the Peng−Robinson[47] equation of state, with binary interaction parameters $k_{ij} = 0$ and without volume translation, the difference between the ϵ_r obtained from method 2 and the ϵ_r(exptl) increased with increasing density from (0.2 and 1.4) %. In the following section we discuss differences between the density obtained from ϵ_r(exptl) and values estimated from equations of state. In view of these differences in ρ the observed variations in ϵ_r are not surprising.

The values of ϵ_r differ, as Figure 6 shows, from all four estimates at $T = 318$ K ($10^3\rho_n \approx 1.4$ mol·cm^{-3}), our lowest, by less than ±0.05 %, which is within the combined uncertainty of our measurements and the literature sources. The estimates obtained from the Schmidt and Moldover[17] method with the mixture density from the Soave−Redlich−Kwong[43] equation of state agree within the experimental uncertainty at all temperatures, but when the mixture density was obtained from the equation of state of Kiselev[44] the deviations increased with increasing temperature to be 0.3 % at $T = 340.07$ K ($10^3\rho_n \approx 3.2$ mol·cm^{-3}) and exhibited a step discontinuity to agree within the stated expanded uncertainty at $T = 343.48$ K ($10^3\rho_n \approx 4.5$ mol·cm^{-3}) close to critical. This agreement is considered to be remarkable because the maximum density of the measurements of ref 17 with propane was limited to ≤0.0004 mol·cm^{-3}, which is 10 times less than the density of our mixture and is one plausible source for the step discontinuity shown in Figure 7.

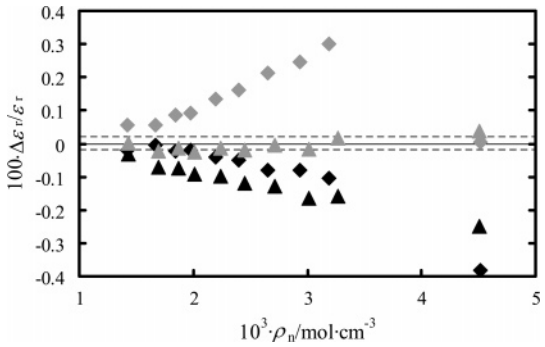

Figure 6. Relative deviations $\Delta\epsilon_r/\epsilon_r = \{\epsilon_r(\text{exptl}) - \epsilon_r(\text{calcd})\}/\epsilon_r(\text{calcd})$ of the experimentally determined relative electric permittivity ϵ_r(exptl) for (0.4026 CH_4 + 0.5974 C_3H_8) listed in Table 1 from the calculated ϵ_r(calcd) as a function of amount of substance density ρ_n at the temperatures and pressures listed in Table 1: gray triangle, ϵ_r(calcd) obtained from the Schmidt and Moldover[17] values of $\mathscr{P}$ for each pure component combined with eq 11 and eqs 5, 6, 7 and ρ_n estimated from the Soave−Redlich−Kwong[43] equation of state with binary interaction parameter $k_{ij} = 0.012$; gray diamond, ϵ_r(calcd) obtained from the Schmidt and Moldover[17] values of $\mathscr{P}$ for each pure component combined with eq 11 and eqs 5, 6, 7 and ρ_n estimated from the Patel and Teja[52,53] type crossover cubic equation of state with $k_{ij} = -0.03606$ adjusted to fit the (p_c, T_c, x) data from the literature by Kiselev;[45,46] ▲, ϵ_r(calcd) obtained from the Harvey and Lemmon[16] correlation given by eqs 8, 12, and 13 and ρ_n estimated from the Soave−Redlich−Kwong[43] equation of state with binary interaction parameter $k_{ij} = 0.012$; ◆, ϵ_r(calcd) obtained from the Harvey and Lemmon[16] correlation given by eqs 8, 12, and 13 and ρ_n estimated from the Patel and Teja[52,53] type crossover cubic equation of state with $k_{ij} = -0.03606$ as reported by Kiselev.[45,46] The dashed lines are the estimated expanded uncertainty of ±0.03 %.

Density of (0.4026 CH_4 + 0.5974 C_3H_8). Two methods were used to estimate the gas-phase amount-of-substance density, $\rho_n(x, \text{exptl})$, for the mixture from the measured relative permittivity ϵ_r(exptl). In the first approach, the total polarizability of the mixture $\mathscr{P}$(0.4026 CH_4 + 0.5974 C_3H_8, p, T) was estimated from the Schmidt and Moldover[17] $\mathscr{P}(\rho_n, T)$ for the pure components (eqs 5 and 6) with parameters from ref 17 and ρ of the pure components from refs 35 and 37, and these values were combined with Oster's mixing rule[19] (eq 11) and ϵ_r(exptl) in eq 7 to give the density of the mixture denoted ρ_n(SM); eq 8 was also used to estimate ρ_n(SM), and the difference between these values and those of Table 1 increased with increasing temperature from (0.1 and 0.6) %. The second method, the Harvey and Lemmon[16] correlation for $\mathscr{P}$(0.4026 CH_4 + 0.5974 C_3H_8, p, T), was used, and the mixture density ρ_n(HL) was determined by iteration until the difference between the calculated and measured permittivity less than 10^{-8}. The critical molar volumes required for this method were taken as $V^c_m(CH_4) = 200$ cm^3·mol^{-1} and $V^c_m(C_3H_8) = 98.629$ cm^3·mol^{-1} from refs 35 and 37, respectively. The values of ρ_n(SM) and ρ_n(HL) are listed in Table 1 at arbitrarily selected temperatures and pressures and differ systematically from 0.6 % at $T = 318.4$ K to 1.8 % at $T = 343.48$ K, which is between (0.8 and 2.3) times the estimated expanded uncertainty (see below). It is plausible the differences arose because of the limitation of Oster's rule that was used in method 1.[16]

The uncertainty in the values of $\rho_n(x, \text{exptl})$ obtained from these two methods has, in the absence of direct measurements, been estimated from measurements of ϵ_r and mass density ρ for (0.8419 CH_4 + 0.1581 C_3H_8) reported by May et al.[14] with standard uncertainties of $\delta\epsilon_r/\epsilon_r = 10^{-4}$ and $\delta\rho = \pm(0.036\ \% + 0.013$ kg·m^{-3}). From these measurements, $\mathscr{P}(x, p, T)$ was determined and compared with the total molar polarizability of the mixture estimated from $\mathscr{P}$(g, CH_4, ρ_n, T) of ref 34 and by extrapolation of $\mathscr{P}$(1, C_3H_8, p, T) obtained from the correlation

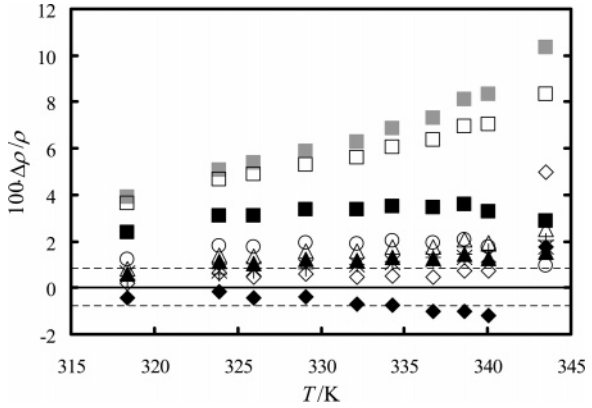

Figure 7. Relative deviations $\Delta\rho/\rho = \{\rho_n(x, \text{calcd}) - \rho_n(\text{exptl})\}/\rho_n(\text{exptl})$ of the experimentally determined amount of substance density $\rho_n(x, \text{exptl})$ for (0.4026 CH_4 + 0.5974 C_3H_8) obtained from the measured $\epsilon_r(x, T, p)$ of Table 1 using eq 14 with $\mathscr{P}(x, \rho_n, T)$ estimated with the Harvey and Lemmon[16] method from ρ(calcd) obtained from equations of state as a function of temperature T: □, Peng−Robinson equation of state with binary interaction parameters $k_{ij} = 0$ as implemented within the software package HYSYS;[44] ■, Peng−Robinson equation of state with $k_{ij} = 0.06$ as implemented within the software package HYSYS;[44] gray square, Peng−Robinson equation of state with volume translation as implemented within the software package VMGThermo;[51] ○, Benedict−Webb−Rubin−Starling equation of state as implemented within VMGTHermo;[51] △, Soave−Redlich−Kwong[43] equation of state with $k_{ij} = 0$ as implemented within the software package HYSYS;[44] ▲, Soave−Redlich−Kwong[43] equation of state with $k_{ij} = 0.012$; ◆, Patel and Teja[52,53] type crossover cubic equation of state with $k_{ij} = -0.03606$ adjusted to fit the literature (p_c, T_c, x) data by Kiselev;[45,46] ◇, Patel and Teja[52,53] type crossover cubic equation of state with $k_{ij} = -0.04113$ adjusted to fit the literature (p, V, T, x) data by Kiselev;[45,46] ∗, values obtained from $\mathscr{P}(x, \rho_n, T)$ estimated with the Schmidt and Moldover[17] values of $\mathscr{P}(\rho_n, T)$ for pure CH_4 and C_3H_8 calculated with eqs 5, 6, and 7 combined according to Oster's rule eq 11 with $\rho_n(CH_4)$ of ref 35 and $\rho_n(C_3H_8)$ of ref 36; +, Younglove and Ely.[33] The dashed lines are the expanded ($k = 2$) uncertainty of ±0.8 % obtained from ref 14.

of Younglove and Ely[33] in the gas phase. Comparison of the measured and calculated $\mathscr{P}$ differed by 0.4 % with an estimated standard uncertainty of ±0.2 %. On the basis of these measurements, and our use of gas phase $\mathscr{P}(C_3H_8, p, T)$, it is reasonable to assume an expanded uncertainty of ±0.8 % for the amount of substance density reported in Table 1. The $<\delta(\rho_n)>$ = 1.1 % between ρ_n(SM) and ρ_n(HL) is another measure of the uncertainty in ρ_n that is within a reasonable multiple (about 1.4 times) of the estimated expanded uncertainty.

Unfortunately, we are not aware of independent measurements of the amount of substance density for (0.4026 CH_4 + 0.5974 C_3H_8) with which to compare the results. Thus, comparisons have been made with values estimated from the following five equations of state: (1) the Starling[48,49] modification of the Benedict−Webb−Rubin equation of state[50] as implemented within VMGThermo;[51] (2) the Peng−Robinson cubic equation of state with and without volume translation;[47] (3) the Soave−Redlich−Kwong[43] cubic equation of state; (4) a cubic crossover equation of state of the Patel and Teja[52,53] type as reported by Kiselev[45] with interaction parameters adjusted to literature values of either (p_c, T_c, x) or (p, V, T, x) by Kiselev;[46] and (5) the modified Benedict−Webb−Rubin equation of state reported by Younglove and Ely.[33] In this work, the Peng−Robinson and Soave−Redlich−Kwong equations of state were implemented in the simulation software known by the acronym HYSYS;[44] the Peng−Robinson cubic equation of state with volume translation and the modified Benedict−Webb−Rubin were contained in the software package known by the acronym VGMThermo.[51] Comprehensive reviews of equations of state can be found in ref 54 and one related specifically to cubic equations in ref 55.

Figure 7 shows the difference between ρ_n obtained from these equations of state and ρ_n(HL). The Soave−Redlich−Kwong equation of state, which was intended to predict the density of gas mixtures, with $k_{ij} = 0.0$ differed from ρ_n(HL) by between (0.9 and 2.6) %, and when $k_{ij} = 0.012$, these differences decreased marginally to be from (0.6 to 1.6) %. The densities estimated from the Peng−Robinson equation of state, with and without volume translation and binary interaction parameters $k_{ij} = 0$, differed with increasing temperature from our results by between (3.6 and 10.3) %; the largest differences were obtained when volume translation was included. When $k_{ij} = 0.06$, the differences reduced to be systematically greater than ρ_n(HL) by up to 3 %. These results are not surprising in view of the criteria used to establish the Peng−Robinson cubic equation of state. The density obtained from the Starling modification of the Benedict−Webb−Rubin equation of state, as implemented within VMGThermo,[51] deviated systematically from the measurements listed in Table 1 by between (1 and 2) %.

Because the measurements were performed within the vicinity of the critical temperature T_c (differences of about 20 K from the estimated T_c), the density was also calculated with a crossover cubic equation of state reported by Kiselev;[45,46] a generalized cubic crossover equation of state with corresponding states extended to mixtures with a field variable model has been reported by Kiselev and Ely[56] but was not used in this work. Kiselev[46] used literature values, independent of our measurements, and obtained $k_{ij} = -0.03606$ and $l_{12} = 0.075$ with the (p_c, T_c, x) data and $k_{ij} = -0.04113$ and $l_{12} = 0.0802$ when (p, V, T, x) data were used. The densities obtained with $k_{ij} = -0.03606$ lie below ρ_n(HL) by between −(0.4 and 1) % and within about 2 times the estimated experimental uncertainties except at $T = 343.48$ K, at which the difference is 1.8 %. Adjustment of k_{ij} to be −0.04113 gave densities at $T \leq 340$ K that differed from ρ_n(HL) by <1 %, but again at $T = 343.48$ K there was a step discontinuity so that the difference was 5.1 %. The Kiselev and Rainwater[57,58] parametric crossover representation of the Helmholtz function with corresponding states, known by the acronym CREOS-97, was also used to estimate the density. These estimates were rather disappointing, with differences from ρ_n(HL) of between (−12 and 14) %. For the sake of clarity, the deviations within ±2 % of the values listed in Table 1 are shown in Figure 8 on an ordinate expanded by a factor of 3.5 over that of Figure 7.

Density is one thermodynamic property that can be estimated with equations of state. The agreement between the values of Table 1 and those obtained from the equations of state should be considered fortuitous, and no particular relevance should be attached to the performance of one equation of state over another based solely on our measurements.

Liquid Volume Fraction. Combination of eqs 16 and 17 provides the expression

$$V(\text{l})/\text{cm}^3 = 214.978\,\frac{[\epsilon_r(x, T, p) - \epsilon_r(\text{g}, T, p)]}{\epsilon_r(1, T, p) - \epsilon_r(\text{g}, T, p)} \qquad (18)$$

to determine the liquid volume V(l) formed in the cavity within the (l + g) region. Equation 18 requires values of the relative permittivity of the two-phase fluid mixture within the phase envelope $\epsilon_r(x, p, \text{T})$ as well as the relative permittivity of both the gas $\epsilon_r(\text{g}, T, p)$ and liquid $\epsilon_r(\text{l}, T, p)$ at the same p and T as the mixture.

The measurements reported in ref 2 were performed along isochors and were sufficient to determine the first onset of liquid

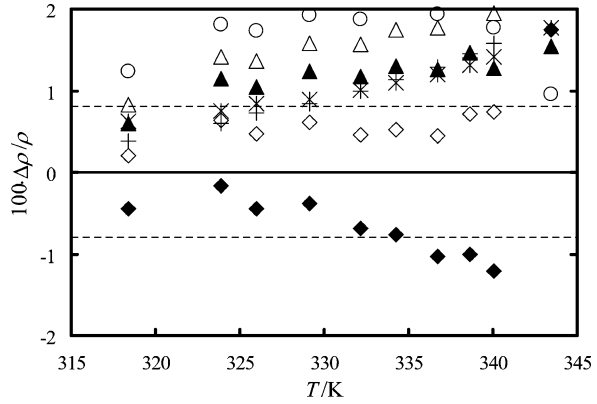

Figure 8. Relative deviations $\Delta\rho/\rho = \{\rho_n(x, \text{calcd}) - \rho_n(\text{exptl})\}/\rho_n(\text{exptl})$ of the experimentally determined amount of substance density $\rho_n(x, \text{exptl})$ for (0.4026 CH_4 + 0.5974 C_3H_8) obtained from the measured $\epsilon_r(x, T, p)$ of Table 1 using eq 14 with $\mathscr{D}(x, \rho_n, T)$ estimated with the Harvey and Lemmon[16] method from ρ(calcd) obtained from equations of state as a function of temperature T: ○, Benedict−Webb−Rubin−Starling equation of state as implemented within VMGTHermo;[51] △, Soave−Redlich−Kwong[43] equation of state with $k_{ij} = 0$ as implemented within the software package HYSYS;[44] ▲, Soave−Redlich−Kwong[43] equation of state with $k_{ij} = 0.012$; ◆, Patel and Teja[52,53] type crossover cubic equation of state with $k_{ij} = -0.03606$ adjusted to fit the (p_c, T_c, x) data from the literature by Kiselev;[45,46] ◇, Patel and Teja[52,53] type crossover cubic equation of state with $k_{ij} = -0.04113$ adjusted to fit (p, V, T, x) data from the literature by Kiselev;[45,46] ∗, values obtained from $\mathscr{D}(x, \rho_n, T)$ estimated with the Schmidt and Moldover[17] values of $\mathscr{D}(\rho_n, T)$ for pure CH_4 and C_3H_8 calculated with eqs 5, 6, and 7 combined according to Oster's rule eq 11 with $\rho_n(CH_4)$ of ref [35] and $\rho_n(C_3H_8)$ of ref 36; +, Younglove and Ely.[33] The dashed lines are the expanded ($k = 2$) uncertainty of ±0.8 % obtained from ref 14.

because it was necessary only to identify the temperature of the phase border from measurements of the resonance frequency. However, because the isochoric measurements were performed with a fixed amount of substance, even near critical, the measurements did not extend through the two-phase region to obtain ϵ_r(l). Thus, $\epsilon_r(l, T, p)$ was obtained from the correlation of ref 16. The $\epsilon_r(g, T, p)$ values were determined from

$$\epsilon_r(g, T, p) = \epsilon_r(g, T^d, p^d) + (p - p^d)\left(\frac{\partial \epsilon_r}{\partial p}\right)_T + (T - T^d)\left(\frac{\partial \epsilon_r}{\partial T}\right)_p \quad (19)$$

In eq 19 $\epsilon_r(g, T^d, p^d)$ was obtained at the dew temperature T^d and pressure p^d from the experimental observations, whereas the derivatives $(\partial\epsilon_r/\partial p)_T$ and $(\partial\epsilon_r/\partial T)_p$ were estimated from the correlation of Harvey and Lemmon;[16] these values were determined from estimates of ϵ_r at no less than five pressures or temperatures, between p and p^d or between T and T^d, within the two-phase region. Unfortunately, the total molar polarizability for each pure component estimated from the Schmidt and Moldover[17] correlation combined with Oster's mixing rule could not be used to verify our estimates of both $\epsilon_r(g, T, p)$ and $\epsilon_r(l, T, p)$ because at our specified T and p the required densities were calculable in the gas phase for methane or in the liquid phase for propane; the densities of propane also far exceeded the upper value used by Schmidt and Moldover.[17] On the basis of the differences between the observed and estimated relative permittivities of the mixture shown in Figure 6 we anticipate the estimated relative permittivities introduced an additional uncertainty of <1 % in our calculated liquid volume fractions.

The volume of liquid formed, V(l), within the (liquid + gas) region was obtained from eq 18 for measurements at temperatures below those assigned to the phase border in ref 2. These

Table 2. Relative Electric Permittivity Obtained Experimentally in the Two-Phase Region ϵ_r(l+g, exptl) and the Gas-Phase ϵ_r(g, exptl) along with the Relative Permittivity Estimated for the Liquid Phase ϵ_r(l, calcd) from Reference 16 with the Density of the Mixture Obtained from the Peng−Robinson Cubic Equation of State Including Volume Translation As Implemented within VMGThermo[51] and the Derived Liquid Volume V(l, exptl) and Liquid Volume Fraction within the Phase Boundary 100V(l, exptl)/V(l+g) at Temperature T and Pressure p for (0.4026 CH_4 + 0.5974 C_3H_8)

T	p				V(l, exptl)	100V(l, exptl)
K	MPa	ϵ_r(l+g, exptl)	ϵ_r(g, exptl)	ϵ_r(l, calcd)	cm^3	V(1 + g)
337.84	6.6681	1.17377	1.16986	1.39	3.73	6.92
335.69	5.5094	1.12418	1.12172	1.47	1.51	2.80
334.50	5.2168	1.11429	1.11365	1.49	0.37	0.68
334.50	5.4464	1.12144	1.11973	1.48	1.02	1.90
333.83	5.1848	1.11295	1.11100	1.49	1.10	2.04
333.83	5.4095	1.11983	1.11693	1.48	1.71	3.16
332.50	4.8403	1.10238	1.10042	1.51	1.03	1.90
332.50	5.1150	1.10964	1.10716	1.50	1.36	2.51
332.50	5.3360	1.11750	1.11251	1.49	2.83	5.25
331.38	4.7881	1.10031	1.09772	1.52	1.33	2.47
331.38	5.0557	1.10789	1.10387	1.51	2.14	3.97
331.38	5.2744	1.11604	1.10890	1.50	3.94	7.30
330.06	4.4746	1.09188	1.09025	1.53	0.79	1.47
330.06	4.7196	1.09744	1.09544	1.52	1.00	1.86
329.11	4.4320	1.09040	1.08837	1.54	0.97	1.80
329.11	4.6728	1.09629	1.09345	1.53	1.40	2.60
326.59	4.1183	1.08199	1.08052	1.56	0.67	1.23
326.59	4.3113	1.08606	1.08423	1.55	0.85	1.57
325.99	4.0907	1.08114	1.07957	1.56	0.70	1.30
325.99	4.2825	1.08539	1.08291	1.55	1.14	2.11
325.07	3.8295	1.07518	1.07437	1.57	0.36	0.66
325.07	4.0489	1.07988	1.07838	1.56	0.67	1.23
324.16	3.7946	1.07442	1.07256	1.57	0.80	1.48
324.16	4.0074	1.07869	1.07639	1.57	1.01	1.87
324.03	3.7945	1.07441	1.07286	1.57	0.67	1.23
324.03	4.0013	1.07855	1.07656	1.57	0.87	1.62
323.01	3.6094	1.06995	1.06961	1.58	0.14	0.27
323.01	3.7450	1.07254	1.07195	1.58	0.25	0.46
322.02	3.5753	1.06921	1.06743	1.59	0.74	1.38
322.02	3.7025	1.07108	1.06959	1.58	0.63	1.16
320.95	3.5304	1.06756	1.06625	1.59	0.54	0.99
320.95	3.6563	1.06951	1.06835	1.59	0.48	0.89
318.15	3.2426	1.06128	1.06031	1.61	0.38	0.71
317.19	3.2046	1.06011	1.05967	1.61	0.17	0.32
316.46	3.1761	1.05924	1.05854	1.61	0.27	0.50
313.04	2.7985	1.05233	1.04982	1.63	0.93	1.72
312.07	2.7645	1.05176	1.04962	1.64	0.79	1.46
311.21	2.7345	1.05131	1.05016	1.64	0.42	0.78

values are listed in Table 2 along with the fraction V(l)/V(l+g) of the total cavity volume V(l+g). To our knowledge there are no values of the liquid volume fraction reported in the literature for our mixture and experimental states with which to compare the values in Table 2. In the absence of independent experimental measurements, we compared our values with those obtained from the Peng−Robinson and Soave−Redlich−Kwong cubic equations of state; the Peng−Robinson without volume translation was implemented with HYSYS,[44] whereas the Peng−Robinson with volume translation was implemented in VMGThermo.[51] The measured liquid volume fractions are, as Figure 9 shows, in agreement with those calculated from the Peng−Robinson equation of state with volume translation, and all but one are within the estimated expanded uncertainty. However, the difference between the experimentally determined liquid volume and that calculated from the Peng−Robinson[47] equation of state, including volume translation, over the liquid volume fractions of ≈(0.004 to 0.058) are, as Figure 10 shows, systematic, with differences from (−1.2 to 1.6) % but within a reasonable multiple of estimated expanded uncertainty 100·δ {V(l)/V(l+g)} ≈ 0.8. The error is about 10 % at V(l)/V(l+g) = 7, and the fractional error increases exponentially with decreasing V(l)/V(l+g) to be about 50 % at V(l)/V(l+g) = 1.6. In view

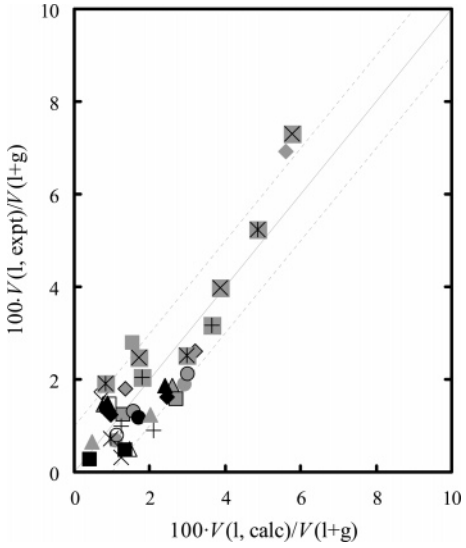

Figure 9. Ratio of the experimentally determined liquid volume V(l, exptl) to the total resonator volume V(l+g) as a function of the ratio of the liquid volume calculated, from the Peng−Robinson[47] equation of state including volume translation using VMGThermo,[51] V(l, calcd) to the total resonator volume V(l+g): ○, T = 311.21 K; □, T = 312.07 K; ◇, T = 313.04 K; △, T = 316.46 K; ×, T = 317.19 K; ∗, T = 318.15 K; +, T = 320.95 K; ●, T = 322.02 K; ■, T = 323.01 K; ◆, T = 324.03 K; ▲, T = 324.16 K; gray triangle, T = 325.07 K; gray solid circle, T = 325.99 K; gray solid square, T = 326.59 K; gray solid diamond, T = 329.11 K; gray solid triangle, T = 330.06 K; cross on gray background, T = 331.38 K; asterisk on gray background, T = 332.50 K; cross on gray background, T = 333.83 K; gray circle, T = 334.50 K; gray square, T = 335.69 K; gray diamond, T = 337.84 K. The dashed lines are the estimated expanded uncertainty $100V$(l)/V(1+g) = ±1.

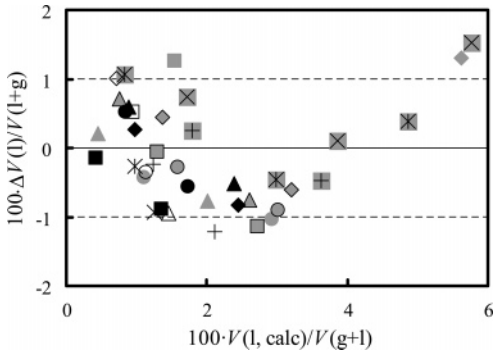

Figure 10. Difference ΔV(l)/V(1+g) = {V(l, exptl) − V(l, calcd)}/V(l+g) of the experimentally determined liquid volume V(l, exptl) from the liquid volume calculated, from the Peng−Robinson[47] equation of state including volume translation using VMGThermo,[51] V(l, calcd) as a ratio of the total resonator volume V(l+g) as a function of the ratio of the calculated liquid volume V(l, calcd) to the total resonator volume V(l+g): ○, T = 311.21 K; □, T = 312.07 K; ◇, T = 313.04 K; △, T = 316.46 K; ×, T = 317.19 K; ∗, T = 318.15 K; +, T = 320.95 K; ●, T = 322.02 K; ■, T = 323.01 K; ◆, T = 324.03 K; ▲, T = 325.07 K; gray triangle, T = 325.07 K; gray solid circle, T = 325.99 K; gray solid square, T = 326.59 K; gray solid diamond, T = 329.11 K; gray solid triangle, T = 330.06 K; cross on gray background, T = 331.38 K; asterisk on gray background, T = 332.50 K; plus on gray background, T = 333.83 K; gray circle, T = 334.50 K; gray square, T = 335.69 K; gray diamond, T = 337.84 K. The dashed lines are the estimated expanded uncertainty $100V$(l)/V(l+g) = ±1.

of these estimated errors the agreement is considered to be remarkable.

The values of the liquid volume fraction V(l, exptl)/V(l+g), where V(l, exptl) is the volume of liquid within the cavity determined from the measured resonance frequency, listed in Table 2, and V(l+g) the total resonator volume, are shown in Figures 11, 12, and 13 as differences from the values predicted

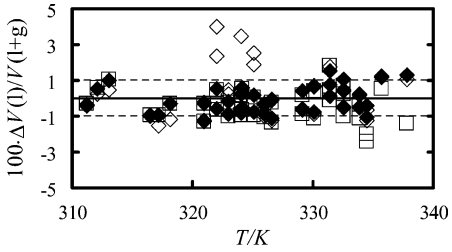

Figure 11. Difference ΔV(l)/V(l+g) = {V(l, exptl) − V(l, calcd)}/V(l+g) of the experimentally determined liquid volume V(l, exptl) from the liquid volume estimated from an equation of state V(l, calcd) divided by the total resonator volume V(l+g) as a function of temperature T: □, V(l, calcd) from the Soave−Redlich−Kwong[43] cubic equation of state as implemented within HYSYS;[44] ◇, V(l, calcd) from the Peng−Robinson[47] cubic equation of state as implemented within HYSYS;[44] ◆, V(l, calcd) from the Peng−Robinson cubic equation of state including volume translation as implemented within VMGThermo.[51] The dashed lines are the estimated expanded uncertainty $100V$(l)/V(l+g) = ±1.

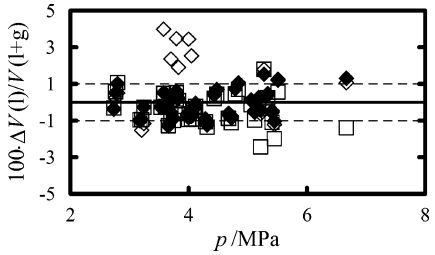

Figure 12. Difference ΔV(l)/V(l+g) = {V(l, exptl) − V(l, calcd)}/V(l+g) of the experimentally determined liquid volume V(l, exptl) from the liquid volume estimated from an equation of state V(l, calcd) divided by the total resonator volume V(l+g) as a function of pressure p: □, V(l, calcd) from the Soave−Redlich−Kwong[43] cubic equation of state as implemented within HYSYS;[44] ◇, V(l, calcd) from the Peng−Robinson[47] cubic equation of state as implemented within HYSYS;[44] ◆, V(l, calcd) from the Peng−Robinson cubic equation of state including volume translation as implemented within VMGThermo.[51] The dashed lines are the estimated expanded uncertainty $100V$(l)/V(1+g) = ±1.

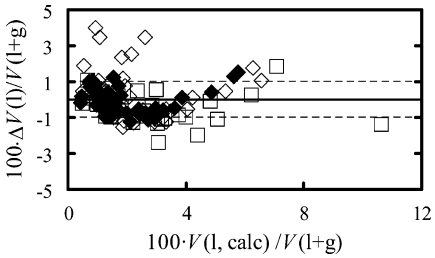

Figure 13. Difference ΔV(l)/V(l+g) = {V(l, exptl) − V(l, calcd)}/V(l+g) of the experimentally determined liquid volume V(l, exptl) from the liquid volume estimated from an equation of state V(l, calcd) divided by the total resonator volume V(l+g) as a function of the ratio of the calculated liquid volume V(l, calcd) to the total resonator volume V(l+g): □, V(l, calcd) from the Soave−Redlich−Kwong[43] cubic equation of state as implemented within HYSYS;[44] ◇, V(l, calcd) from the Peng−Robinson[47] cubic equation of state as implemented within HYSYS;[44] ◆, V(l, calcd) from the Peng−Robinson cubic equation of state including volume translation as implemented within VMGThermo.[51] The dashed lines are the estimated expanded uncertainty $100V$(l)/V(l+g) = ±1.

from the following three equations of state: (1) Soave−Redlich−Kwong cubic equation of state with k_{ij} = 0.012;[43,54] (2) the Peng−Robinson cubic equation of state with k_{ij} = 0.012;[44,47] and (3) the Peng−Robinson cubic equation of state including volume translation with k_{ij} = 0.012.[47,51] Figure 11 shows ΔV(l)/V(l+g) = {V(l, exptl) - V(l, calcd)}/V(l+g) as a function of temperature; Figure 12 shows ΔV(l)/V(l+g) as a function of pressure, wheres Figure 13 shows ΔV(l)/V(l+g) as a function of V(l, calcd)/V(l+g). Not surprisingly, the values

estimated from equation of state 3 agree with the measurements within a small (<0.5 times) deviation of the estimated expanded uncertainty of our measurements. In all three figures, the estimates obtained from equation of state 1 provide values of $100\Delta V(l)/V(l+g)$ that deviate by between −2.5 and 2 (about twice the uncertainty), whereas those from method 2 of $100\Delta V(l)/V(l+g)$ differ by between −1.5 and 4. Nevertheless, the $100\Delta V(l)/V(l+g)$ shown in Figure 13, as a function of $V(l, calcd)/V(l+g)$, have a systematic undulation, albeit for equation of state 3 within the assigned uncertainty. All of these differences are perhaps, in light of the differences shown in Figures 7 and 8 for density, rather surprising.

Acknowledgment

We thank Allan Harvey, National Institute of Standards and Technology, Sergei Kiselev, Colorado School of Mines, and Marco Satyro, Virtual Materials Group, for helpful discussions.

Literature Cited

(1) Kandil, M.; Marsh, K. N.; Goodwin, A. R. H. A Vibrating Wire Viscometer with Wire Diameters of (0.05 and 0.15) mm: Results for Methylbenzene and Two Fluids with Nominal Viscosities at $T = 298$ K and $p = 0.01$ MPa of (14 and 240) mPa·s at Temperatures between (298 and 373) K and Pressures below 40 MPa. *J. Chem. Eng. Data* **2005**, *50*, 647−655.

(2) Kandil, M. E.; Marsh, K. N.; Goodwin, A. R. H. A re-entrant resonator for the measurement of phase boundaries: dew points for $\{0.4026CH_4 + 0.5974C_3H_8\}$. *J. Chem. Thermodyn.* **2005**, *37*, 684−691.

(3) Dandekar, A. Y.; Stenby, E. H. Measurement of Phase Boundaries of Hydrocarbon Mixtures Using Fiber Optical Detection Techniques. *Ind. Eng. Chem. Res.* **2000**, *3*, 2586−2591.

(4) Goodwin, A. R. H.; Froerup, M. D.; Stenby, E. H. Microwave detection of dew points: results for complex mixtures. *J. Chem. Thermodyn.* **1991**, *23*, 713−715.

(5) Burfield, D. W.; Richarson, H. P.; Guereca, R. A. Vapor−liquid equilibria and dielectric constants for the helium−carbon dioxide system. *AIChE J.* **1970**, *16*, 97−100.

(6) Chan, M.; Ryschkewitsch, H. P.; Meyer, H. Dielectric Constant in Liquid and Solid He-4. *J. Low Temp. Phys.* **1977**, *26*, 211−228.

(7) St-Arnaud, J. M.; Bose, T. K.; Okambawa, R.; Ingrain, D. Application of the dielectric constant measurements to study the influence of the small quantities of water vapour on the compressibility factor of methane. *Int. J. Thermophys.* **1992**, *13*, 685−697.

(8) Goodwin, A. R. H.; Mehl, J. B.; Moldover, M. R. Reentrant radio-frequency resonator for automated phase-equilibria and dielectric measurements in fluids. *Rev. Sci. Instrum.* **1996**, *67*, 4294−4304.

(9) Goodwin, A. R. H.; Moldover, M. R. Phase border and density determinations in the critical region of (carbon dioxide + ethane) determined from dielectric permittivity measurements. *J. Chem. Thermodyn.* **1997**, *29*, 1481−1494.

(10) Hamelin, J.; Mehl, J. B.; Moldover, M. R. Resonators for accurate dielectric measurements in conducting liquids. *Rev. Sci. Instrum.* **1998**, *69*, 255−260.

(11) Hamelin, J.; Mehl, J. B.; Moldover, M. R. The static dielectric constant of liquid water between 274 and 418 K near the saturated vapour pressure. *Int. J. Thermophys.* **1998**, *19*, 1359−1380.

(12) Anderson, G. S.; Miller, R. C.; Goodwin, A. R. H. Static dielectric constants for liquid water from 300 K to 350 K at pressures to 13 MPa using a new radio-frequency resonator. *J. Chem. Eng. Data* **2000**, *45*, 549−554.

(13) Goodwin, A. R. H.; Mehl, J. B. Measurements of the dipole moments of seven partially fluorinated hydrocarbons with a radiofrequency re-entrant cavity resonator. *Int. J. Thermophys.* **1997**, *18*, 795−806.

(14) May, E. F.; Miller, R. C.; Goodwin, A. R. H. Dielectric Constants and Molar Polarizabilities for Vapor Mixtures of Methane + Propane and Methane + Propane + Hexane Obtained with a Radio Frequency Reentrant Cavity. *J. Chem. Eng. Data* **2002**, *47*, 102−105.

(15) May, E. F.; Edwards, T. J.; Mann, A. G.; Edwards, C. Dew point, liquid volume, and dielectric constant measurements in a vapour mixture of methane + propane using a microwave apparatus. *Int. J. Thermophys.* **2003**, *24*, 1509−1525.

(16) Harvey, A. H.; Lemmon, E. W. Methods for the dielectric constant of natural gas mixtures. *Int. J. Thermophys.* **2005**, *26*, 31−46.

(17) Schmidt, J. W.; Moldover, M. R. Dielectric permittivity of eight gases measured with cross capacitors. *Int. J. Thermophys.* **2003**, *24*, 375−403.

(18) Harvey, A. H.; Prausnitz, J. M. Dielectric constant of fluid mixtures over a wide range of temperature and density. *J. Solution Chem.* **1987**, *16*, 857−869.

(19) Oster, G. The dielectric properties of liquid mixtures. *J. Am. Chem. Soc.* **1946**, *68*, 2036− 2041.

(20) Moldover, M. R.; Marsh, K. N.; Barthel, J.; Buchner, R. Relative Permittivity and Refractive Index. In *Experimental Thermodynamics Vol. VI, Measurement of the Thermodynamic Properties of Single Phases*; Goodwin, A. R. H., Marsh, K. N., Wakeham, W. A., Eds.; for International Union of Pure and Applied Chemistry, Elsevier: Amsterdam, The Netherlands, 2003; Chapter 9, pp 127−235.

(21) Marcuwitz, N. *Waveguide Handbook*; McGraw-Hill: New York, 1951; Section 5.27

(22) Straty, G. C.; Goodwin, R. D. Dielectric constant and polarizability of saturated and compressed fluid methane. *Cryogenics* **1973**, *13*, 712−715.

(23) Bell, R. P. Polarizibility and internuclear distance. *Trans. Faraday Soc.* **1942**, *38*, 422−429.

(24) Haynes, W. M. Measurements of densities and dielectric constants of liquid propane from 90 to 300 K at pressures to 35 MPa. *J. Chem. Thermodyn.* **1983**, *15*, 419−424.

(25) Haynes, W. M.; Younglove, B. A. In *Advancss in Cryogenic Engineering*; Fast, R. W., Ed.; Plenum Press: New York, 1982; Vol. 27, p 883.

(26) Haynes, W. M. Measurements of Densities and Dielectric Constants of Liquid Isobutane from 120 to 300 K at Pressures to 35 MPa. *J. Chem. Eng. Data* **1983**, *28*, 367−369.

(27) Böttcher, C. J. F. *Theory of Electric Polarization*, 2nd ed.; Elsevier: Amsterdam, The Netherlands, 1973; Vol. 1.

(28) Kirkwood, J. G. The Dielectric Polarization of Polar Liquids. *J. Chem. Phys.* **1939**, *7*, 911− 919.

(29) Hirschfelder, J. P.; Curtiss, C. F.; Bird, R. B. *Molecular Theory of Gases and Liquids*; Wiley: New York. 1954; p 858.

(30) Haynes, W. M. Orthobaric liquid densities and dielectric constants of (methane + 2-methylpropane) and (methane + *n*-butane) at low temperatures. *J. Chem. Thermodyn.* **1983**, *15*, 903−911.

(31) Luo, C. C.; Miller, R. C. Densities and dielectric constants for some LPG components and mixtures at cryogenic and standard temperatures. *Cryogenics* **1981**, *21*, 85−93.

(32) May, E. F.; Miller, R. C.; Shan, J. Densities and Dew-Points of Vapour Mixtures of Methane + Propane and Methane + Propane + Hexane Using a Dual-Sinker Densimeter. *J. Chem. Eng. Data* **2001**, *46*, 1160−1166.

(33) Younglove, B. A.; Ely, J. F. Thermophysical Properties of Fluids. II. Methane, Ethane, Propane, Isobutane and Normal Butane. *J. Phys. Chem. Ref. Data* **1987**, *16*, 577−582.

(34) Moldover, M. R.; Buckley, T. J. Reference Values of the Dielectric Constant of Natural Gas Components Determined with a Cross Capacitor. *Int. J. Thermophys.* **2001**, *22*, 859−885.

(35) Setzmann, U.; Wagner, W. A. New Equation of State and Tables of Thermodynamic Properties for Methane Covering the Range from the Melting Line to 625 K at Pressures up to 1000 MPa. *J. Phys. Chem. Ref. Data* **1991**, *20*, 1061−1151.

(36) Trusler, J. P. M. Equation of state for gaseous propane determined from the speed of sound. *Int. J. Thermophys.* **1997**, *18*, 635−654.

(37) Span, R.; Wagner, W. Equations of State for Technical Applications. II. Results for Nonpolar Fluids *Int. J. Thermophys.* **2003**, *24*, 41−109.

(38) *ASM Metals Reference Book*; Bauccio, M., Ed.; ASM International: Materials Park, OH, 1993.

(39) Lemmon, E. W.; McLinden, M. O.; Huber, M. L. *NIST Standard Reference Database 23 version 7.1 (REFPROP)*; National Institute of Standards and Technology: Gaithersburg, MD, 2004.

(40) Maryott, A. A.; Smith, E. R. *Table of Dielectric Constants of Pure Liquids*; National Bureau of Standards Circular 514; U.S. GPO: Washington, DC, 1951.

(41) Scaife, W. G.; Lyons, C. G. R. *Proc. R. Soc. London A* **1980**, *370*, 193.

(42) Scaife, W. G.; Lyons, C. G. R. An equation of state based on measurements of relative dielectric permittivity. *J. Phys. D: Appl. Phys.* **1983**, *16*, 39−52.

(43) Soave, G. Equilibrium Constants from a Modified Redlich-Kwong Equation of State. *Chem. Eng. Sci.* **1972**, *27*, 1197−1203.

(44) HYSYS version 3.2; Aspentech, Boston, MA, 2003.

(45) Kiselev, S. B. Cubic crossover equation of state. *Fluid Phase Equilib.* **1998**, *147*, 7−23.

(46) Kiselev, S. B. Colorado School of Mines, Golden, CO; personal communication, 2004.

(47) Peng, D.-Y.; Robinson, D. B. A New Two-constant Equation of State. *Ind. Eng. Chem. Fundam.* **1976**, *15*, 59−64.

(48) Cox, K. W.; Bono, J. L.; Kwok, Y. C.; Starling, K. E. Multiproperty Analysis. Modified BWR Equation for Methane from PVT and Enthalpy Data. *Ind. Eng. Chem. Fundam.* **1971**, *10*, 245−250.
(49) Starling, K. E. *Fluid Thermodynamic Properties for Light Petroleum Systems*; Gulf Publishing: Mobile, AL,1973.
(50) Benedict, M.; Webb, G. B.; Rubin, L. C. An Empirical Equation for Thermodynamic Properties of Light Hydrocarbons and Their Mixtures: I. Methane, Ethane, Propane, and n-Butane. *J. Chem. Phys.* **1940**, *8*, 334−345.
(51) Thermodynamics package VMGThermo, V 2.8.0; Virtual Materials Group, Calgary, AB, Canada.
(52) Patel, N. C.; Teja, A. S. A new Cubic Equation of State for Fluids and Fluid Mixtures. *Chem. Eng. Sci.* **1982**, *37*, 463−473.
(53) Patel, N. C. Improvement of the Patel−Teja equation of state. *Int. J. Thermophys.* **1996**, *17*, 673−680.
(54) Reid, R. C.; Prausnitz, J. M.; Poling, P. E. *The Properties of Gases and Liquids*, 4th ed.; McGraw-Hill: New York, 1986.
(55) Twu, C. H.; Sim, W. D.; Tassone, V. *Getting a Handle on Advanced Cubic Equations of State. Measurement & Control*; Aspen Technology: Bothell, WA, 2002; pp 58−65.
(56) Kiselev, S. B.; Ely, J. F. Generalized corresponding state model for bulk and interfacial properties in pure fluids and fluid mixtures. *J. Chem. Phys.* **2003**, *119*, 8645−8662.
(57) Kiselev, S. B.; Rainwater, J. C. Extended law of corresponding states and thermodynamic properties of binary mixtures beyond the critical region. *Fluid Phase Equlib.* **1997**, *141*, 129− 154.
(58) Kiselev, S. B.; Rainwater, J. C. Enthalpies, excess volumes, and specific heats of critical and supercritical binary mixtures *J. Chem. Phys.* **1998**, *109*, 643−657.

Received for review January 31, 2007. Accepted June 16, 2007.

JE700053U